

Morphology of M (3000) F2 And Its Relationship with Solar Flux (F10.7) At an African Equatorial Sector

AFOLABI PETERS ABIODUN (Ph.D)

*Department of Physics
Kwara State College of Education, Oro*

Date of Submission: 13-02-2026

Date of Acceptance: 25-02-2026

Abstract

This research examined the morphological characteristics of the propagation parameter M(3000)F2 and its association with solar activity, represented by the solar flux index F10.7, using archival data obtained from the equatorial ionosonde station at Korhogo, Côte d'Ivoire. The analysis was based on previously published datasets covering the period from January 1993 to December 2000. Hourly and monthly averaged values of M(3000)F2 were evaluated in order to assess its diurnal, seasonal, and interannual behavior. For seasonal analysis, the data were classified into equinoctial and solstitial periods, while linear regression techniques were applied to determine the extent of the relationship between M(3000)F2 and solar flux. The findings revealed that M(3000)F2 displayed marked diurnal fluctuations, with pronounced peaks around sunrise, clearly defined daytime minima, notable post-sunset increases, and strong nighttime maxima across all seasons. On a seasonal scale, M(3000)F2 values were consistently higher during the equinoxes than during the solstices, suggesting stronger equatorial electrodynamic processes during equinoctial intervals. The interannual assessment further indicated that elevated M(3000)F2 values were more prevalent during periods of low solar activity, whereas reduced values corresponded with years of high solar activity. The regression analysis confirmed a persistent inverse relationship between M(3000)F2 and the solar flux index across all seasons, as evidenced by negative regression slopes and statistically significant correlation coefficients, particularly during daylight hours. Overall, the

results demonstrated that solar activity plays a major role in controlling the long-term variation of M(3000)F2, while equatorial electrodynamic mechanisms significantly influence its diurnal and seasonal patterns. This study offers valuable empirical insight from a relatively underexplored African equatorial region and enhances understanding of ionospheric propagation conditions relevant to high-frequency radio communication and ionospheric modeling in West Africa.

Keywords: M(3000)F2; Solar flux (F10.7); Equatorial ionosphere; HF radio propagation; Korhogo ionosonde

I. Introduction

The ionosphere is fundamental to long-distance high-frequency (HF) radio communication, satellite signal transmission, navigation systems, and space-weather surveillance. Within the ionospheric structure, the F2 layer is particularly significant for HF communication because it possesses the highest electron density and enables long-range sky-wave propagation¹. Among the parameters commonly employed to describe the characteristics of the F2 layer is the M(3000)F2 propagation factor. This parameter represents the ratio of the Maximum Usable Frequency (MUF) over a 3000 km radio path to the critical frequency of the F2 layer (f_oF2)² and can be expressed mathematically as:

$$M(3000)F2 = \frac{MUF(3000)}{f_oF2} \quad (1)$$

The M(3000)F2 parameter is commonly employed as an indirect indicator of the effective height, structural configuration, and curvature of the ionospheric F2 layer. Consequently, it responds strongly to variations in ionospheric processes, including electric field dynamics, thermospheric wind circulation, magnetic field orientation, and changes in solar irradiance³. An examination of its morphological characteristics offers valuable understanding of the ionosphere's reaction to different geophysical drivers, especially within equatorial and low-latitude regions where distinctive electrodynamic mechanisms prevail.

The Maximum Usable Frequency (MUF) refers to the uppermost radio frequency that can reliably propagate over a given distance through ionospheric refraction. For a transmission path of 3000 km, the MUF is closely associated with:

$$MUF(3000) = M(3000)F2 \times f_oF2(2)$$

An increase in the Maximum Usable Frequency (MUF) is generally associated with several ionospheric and solar-related conditions. These include elevated electron density in the F2 layer, reflected by higher foF2 values, increased peak height of the F2 layer (hmF2) which enhances the refraction path length, intensified solar radiation as indicated by elevated F10.7 index values, and seasonal amplification during equinoctial periods. A clear understanding of MUF behavior and its controlling factors is essential for maintaining reliable radio communication, particularly in regions with limited satellite coverage or where high-frequency (HF) communication remains operationally critical, such as in military, maritime, and aviation applications.

Beyond internal plasma processes, the ionosphere is strongly modulated by solar activity,

which is commonly quantified using the F10.7 cm solar radio flux index. This index represents solar emissions measured at a wavelength of 10.7 cm and has been shown to correlate closely with extreme ultraviolet (EUV) radiation, the primary driver of ionization in the F2 layer⁴. Fluctuations in F10.7 are therefore recognized as key drivers of long-term, annual, seasonal, and daily variations in M(3000)F2, as well as other fundamental ionospheric parameters such as foF2 and hmF2⁵.

The African equatorial ionosphere displays distinctive characteristics arising from intense equatorial electric fields, the influence of magnetic declination, and the presence of the equatorial ionization anomaly (EIA). These factors give rise to spatial and temporal ionospheric behaviors that often differ markedly from those observed in equatorial regions of Asia, the Americas, and the Pacific⁶. Korhogo, located in Ivory Coast at approximately 9.33°N latitude and 5.42°W longitude, constitutes a key ionospheric observation site within the West African low-latitude zone. The station offers valuable long-term ionosonde measurements that are crucial for investigating F2-layer variability and propagation conditions in this region.

A detailed understanding of the morphological behavior of M(3000)F2 in relation to solar flux is vital for effective HF communication planning, mitigation of space-weather impacts, and optimization of radio-frequency systems across the African continent. Additionally, analyses spanning extended intervals, such as the period from 1993 to 2000 corresponding largely to solar cycle 23, provide a more comprehensive framework for assessing the response of equatorial ionospheric parameters under varying levels of solar activity.

Statement of the Problem

Although the African equatorial ionosphere plays a significant role in global radio communication systems, it remains comparatively underrepresented in ionospheric research when contrasted with equatorial regions in the Americas and Asia. In particular, the characteristics and variability of M(3000)F2 in West Africa, and its sensitivity to changes in solar activity, are not yet fully understood. While previous investigations have been conducted at stations such as Ouagadougou, Addis Ababa, and Lagos, relatively few studies have concentrated on Korhogo, despite its advantageous position within the equatorial ionization anomaly region^{7,8}

Moreover, the quantitative relationship between solar flux, as represented by the F10.7 index, and M(3000)F2 over long observational periods in the African sector remains inadequately documented. Existing evidence suggests that equatorial electrodynamic processes may introduce nonlinear or season-dependent responses of M(3000)F2 to solar forcing⁹. However, comprehensive and continuous multi-year observations from Korhogo are limited and often fragmented. This highlights the need for a systematic investigation that examines the long-term morphology of M(3000)F2, evaluates its diurnal and seasonal behavior, and rigorously quantifies its dependence on solar flux (F10.7) within the African low-latitude ionosphere.

Aim of the Study

The central objective of this research is to analyze the morphological characteristics of the propagation parameter M(3000)F2 and to assess its relationship with solar activity, as measured by the F10.7 index, at the African equatorial ionosonde

station of Korhogo over the period spanning January 1993 to December 2000.

Objectives of the Study

The study is designed to achieve the following specific objectives:

- i. To investigate the diurnal and seasonal patterns of variation of the M(3000)F2 propagation factor at Korhogo over the period 1993–2000.
- ii. To assess the long-term behavior of M(3000)F2 in relation to the different phases of solar cycle 23.
- iii. To evaluate the relationship between solar activity, represented by the F10.7 index, and M(3000)F2 by examining correlation strength and response characteristics.
- iv. To provide a scientific explanation of the physical processes responsible for the observed variations in M(3000)F2 at the Korhogo station.

Justification of the Study

A detailed investigation of the morphology of M(3000)F2 and its dependence on solar flux (F10.7) within the African equatorial region is of considerable scientific and practical significance. The West African equatorial ionosphere is distinguished by complex features such as the equatorial ionization anomaly (EIA), intense electrodynamic drifts, rapid plasma irregularities, and pronounced day–night variability. These characteristics pose substantial challenges to high-frequency radio propagation, satellite-based navigation systems, remote sensing, and other space-dependent technologies operating in the region. Nevertheless, sustained and location-specific ionospheric observations across West Africa remain limited, resulting in persistent uncertainties in regional ionospheric modeling and forecasting.

Korhogo lies within the equatorial ionospheric zone and represents one of the few stations providing long-term ionosonde observations in this part of Africa. Consequently, it offers a valuable opportunity to examine F2-layer behavior in a region where observational data are scarce. Many widely used ionospheric models, including the International Reference Ionosphere (IRI), NeQuick, and SUPIM, are largely constrained by datasets from mid-latitude regions and equatorial sectors in America and Asia. As a result, their performance over the African equatorial sector is often suboptimal. An empirical analysis of M(3000)F₂ based on Korhogo ionosonde measurements from 1993 to 2000 therefore contributes to narrowing this data gap and improving the representation of African equatorial conditions in both global and regional ionospheric models.

In addition, the F10.7 solar flux index remains a standard proxy for solar extreme ultraviolet (EUV) radiation, which is the primary source of ionization in the upper atmosphere. However, the magnitude, timing, and linearity of ionospheric responses to solar flux vary with latitude and local electrodynamic conditions. Evidence from previous studies suggests that equatorial ionospheric parameters often display nonlinear and seasonally dependent responses to solar forcing, yet such behavior has not been sufficiently documented for the longitude sector encompassing Korhogo. A long-term analysis covering the interval 1993–2000, which includes periods of both moderate and elevated solar activity, provides a robust framework for understanding how solar cycle variability influences HF propagation characteristics in this region.

Accurate knowledge of M(3000)F₂ variability is essential for effective frequency

planning and operational reliability in sectors such as military communications, emergency response, aviation routing, and broadcasting services that depend on ionospheric propagation. Furthermore, as sub-Saharan Africa increasingly adopts GNSS-based technologies for navigation, surveying, and emerging autonomous applications, improved understanding of equatorial ionospheric dynamics becomes increasingly critical.

Finally, the limited availability of long-term ionospheric observations from the pre-digital ionosonde era, including datasets spanning 1993–2000, underscores the importance of preserving and analyzing historical records. Such data enable the assessment of solar-cycle-related variability, support the validation and calibration of predictive models, and provide a baseline for comparing past ionospheric behavior with contemporary trends under evolving space-weather conditions. The present study is therefore justified on the grounds that it addresses a clear scientific gap, enhances regional modeling capabilities, supports practical communication and navigation needs, and contributes to the broader understanding of equatorial ionospheric physics using underutilized African observational data.

II. Literature Review

Conceptual Review

The ionosphere constitutes a region of the Earth's upper atmosphere extending roughly from about 60 km to beyond 1000 km in altitude and is characterized by significant populations of free electrons and ions generated primarily through photoionization driven by solar extreme ultraviolet (EUV) and X-ray radiation^{10,11}. From a structural perspective, the ionosphere is conventionally divided into the D, E, F1, and F2 layers, each defined by

distinct electron density distributions and differing roles in radio-wave propagation¹.

Among these regions, the F2 layer is the most critical for high-frequency (HF) communication because it attains the highest electron densities and is capable of refracting HF radio signals back to the Earth over long distances. Key parameters describing the F2 layer include the critical frequency (f_oF2), the peak height ($hmF2$), and the maximum electron density ($NmF2$). These parameters are highly variable and are controlled by a combination of solar radiation intensity, geomagnetic conditions, and thermospheric and electrodynamic processes. As a result, the F2 layer represents both the most dynamic and the most operationally significant part of the ionosphere for long-range radio communication¹².

$$f_oF2 = 9 \sqrt{NmF2} \quad (3)$$

- **foF2 (Critical Frequency):** denotes the maximum frequency that can be reflected back to the Earth during vertical incidence by the F2 layer of the ionosphere.
- **NmF2:** corresponds to the peak electron density of the F2 layer and is mathematically linked to f_oF2 , such that variations in f_oF2 directly reflect changes in $NmF2$.
- **hmF2:** refers to the altitude at which the maximum electron density occurs within the F2 region. Fluctuations in $hmF2$ play a significant role in shaping the value and variability of the $M(3000)F2$ propagation factor.
- **h'F2:** represents the virtual height of reflection of the F2 layer as derived from ionogram measurements, providing an apparent reflection height rather than the true physical altitude.

The propagation parameter $M(3000)F2$ is an empirically derived index used to evaluate the effectiveness of high-frequency (HF) radio wave transmission over a standard distance of 3000 km. It is defined as the ratio of the maximum usable frequency for a 3000 km circuit to the critical frequency of the F2 layer (f_oF2). In practical terms, $M(3000)F2$ encapsulates how efficiently the ionosphere can refract HF signals under prevailing geophysical conditions^{2,3}. Since both MUF and f_oF2 are governed by the vertical distribution and magnitude of electron density in the F2 region, variations in $M(3000)F2$ directly reflect changes in ionospheric structure and dynamics. The parameter is particularly valuable because it conveys information about the curvature and height profile of the electron density distribution, making it a reliable indicator of temporal changes in HF propagation conditions driven by solar and geomagnetic influences¹³.

Solar activity exerts a strong influence on ionospheric ionization, commonly represented by the F10.7 cm solar radio flux index. The F10.7 index measures solar radio emissions at a wavelength of 10.7 cm and is widely accepted as a proxy for solar extreme ultraviolet (EUV) radiation, which is primarily responsible for ion production in the F2 layer⁴. Numerous investigations have demonstrated close associations between F10.7 and key ionospheric parameters such as f_oF2 , $hmF2$, and $NmF2$, with elevated solar flux levels generally corresponding to increased electron densities and higher F2-layer peak altitudes, particularly during geomagnetically quiet conditions^{6,14}. Since $M(3000)F2$ depends jointly on f_oF2 and the vertical structure of the F2 layer, it is expected to exhibit systematic responses to solar flux variations, underscoring the relevance of F10.7 in HF propagation analysis and ionospheric modelling.

The equatorial ionosphere is distinguished from mid- and high-latitude regions by a range of unique electrodynamic and structural features. Foremost among these is the equatorial ionization anomaly (EIA), which manifests as two bands of enhanced electron density located roughly $\pm 15^\circ$ from the magnetic equator. This phenomenon is produced by the plasma fountain effect, whereby strong daytime eastward electric fields generate upward $E \times B$ plasma drifts that lift ionospheric plasma to higher altitudes, from where it diffuses along geomagnetic field lines toward lower latitudes^{15,16}. Another defining feature is the equatorial electrojet (EEJ), a narrow and intense eastward current flowing near the magnetic equator that modulates ionospheric electrodynamics and influences parameters such as foF2 and hmF2¹⁷. These processes, together with pronounced diurnal, seasonal, and solar-cycle variability, are especially prominent in low-latitude regions over Africa and play a central role in shaping the morphology of M(3000)F2.

Across longitudes spanning approximately 20°W to 60°E, the African equatorial ionosphere exhibits characteristics that often differ from those observed in other equatorial sectors. Longitudinal variations in electric fields, thermospheric wind systems, and magnetic declination contribute to region-specific F2-layer behaviour^{18,19}. Despite this, the African equatorial region has historically been under-instrumented compared with better-studied areas such as South America and Southeast Asia. As a result, observationally based investigations of propagation parameters like M(3000)F2 remain particularly valuable for improving regional understanding and enhancing the performance of global ionospheric models^{12,20}.

Theoretical Review

The physical behaviour of the ionosphere and its response to external forcing mechanisms are grounded in several established theoretical frameworks. Central to these is Chapman layer theory, which describes the vertical distribution of ionization resulting from the balance between solar photoionization and recombination processes. Developed by Sydney Chapman in the early twentieth century, the theory predicts a characteristic ionization profile in which electron density increases exponentially with altitude to a maximum before decreasing due to enhanced recombination and diffusion^{21,22}. Although simplified, this framework provides a foundational understanding of how ionospheric layers form and vary with solar zenith angle, offering insight into the behaviour of foF2 and related parameters.

Complementing this is solar–terrestrial interaction theory, which explains how changes in solar radiation, solar wind conditions, and geomagnetic activity influence the Earth’s upper atmosphere. Periods of heightened solar EUV and X-ray emissions lead to increased ion production, raising electron densities and altering ionospheric layer heights¹¹. Transient solar phenomena such as solar flares and coronal mass ejections can further introduce rapid and sometimes severe disturbances in the F2 region²³. Over longer timescales, the approximately 11-year solar cycle imposes a systematic modulation on ionospheric parameters, with higher foF2 and MUF values typically occurring near solar maximum²⁴.

The distinctive nature of the equatorial ionosphere is further explained by plasma electrodynamics theory. Vertical plasma drifts driven by $E \times B$ electric fields, in combination with

thermospheric winds and the equatorial electrojet, give rise to the plasma fountain effect and the development of the EIA^{25,26}. These mechanisms exert strong control over hmF2 and NmF2, which in turn influence the refractive properties of the ionosphere relevant to HF propagation. In particular, the pre-reversal enhancement (PRE) of vertical drift near sunset has been shown to cause rapid uplift of the F2 layer, increasing MUF and significantly modifying M(3000)F2 values⁹. The interplay of electric fields, neutral winds, and diffusion processes renders equatorial ionospheric behaviour especially complex and highly sensitive to both solar and geomagnetic forcing.

Radio wave propagation through the ionosphere is fundamentally governed by refractive index theory. According to the Appleton–Hartree formulation, the refractive index of an ionized medium depends on electron density and signal frequency, determining whether HF waves are refracted back toward the Earth or escape into space². Consequently, the maximum usable frequency for a given radio path is closely tied to the peak electron density and curvature of the ionospheric profile, with M(3000)F2 serving as a practical empirical indicator of these conditions. Global ionospheric models, including the International Reference Ionosphere (IRI), incorporate these theoretical principles to provide climatological descriptions of ionospheric parameters¹². However, such models often perform less accurately in equatorial regions, where sparse observations and complex electrodynamics limit predictive reliability²⁷, reinforcing the need for region-specific empirical studies.

Empirical Review

A substantial body of empirical research has examined F2-layer behaviour and related propagation parameters across different latitude regions. These studies consistently show that equatorial ionospheric parameters exhibit distinctive diurnal, seasonal, and solar-cycle characteristics compared with those at higher latitudes.

Within West Africa, early ionosonde-based investigations documented pronounced diurnal and seasonal variability in F2-layer parameters. A study analysed foF2 and hmF2 over Korhogo and reported notable evening uplifts in hmF2 associated with pre-reversal enhancement⁷. Subsequent studies confirmed that equatorial electrodynamic processes exert strong control over F2-layer morphology, particularly during equinoctial periods²⁸. Comparative analyses further demonstrated that African equatorial stations display greater variability than mid-latitude counterparts, especially during seasonal transitions⁸.

Although fewer studies have focused explicitly on M(3000)F2 in Africa, available evidence highlights the combined influence of solar activity and equatorial dynamics. Studies reported well-defined diurnal cycles and seasonal modulation of M(3000)F2 at Ouagadougou, attributing these patterns to variations in hmF2 and NmF2 driven by solar flux and vertical plasma transport²⁸. Another study working with data from Lagos, observed elevated M(3000)F2 values during periods of increased solar activity, supporting the notion of strong solar control at low latitudes²⁹.

Observations from other equatorial regions provide useful comparative insights. A study showed that post-sunset enhancements in hmF2 at Jicamarca significantly increase MUF and M(3000)F2⁹. Studies

in East Africa similarly reported strong correlations between foF2 and F10.7, particularly during high solar activity conditions³¹. On a global scale, assessments of ionospheric models reveal systematic underestimation of equatorial F2-layer parameters, leading to discrepancies in predicted MUF and M(3000)F2 values^{12,31}.

Collectively, the literature indicates that M(3000)F2 exhibits pronounced diurnal and seasonal behaviour influenced by equatorial electrodynamics, while solar flux remains the dominant driver of long-term variability. Persistent discrepancies between observations and model predictions in equatorial regions, especially over Africa, further emphasize the importance of station-specific analyses such as the present investigation at Korhogo.

III. Methodology

Data Used

This study utilizes ionospheric and solar datasets obtained from established and internationally recognized sources to examine long-term variability in the equatorial F2 layer over Korhogo. The analysis covers the period from January 1993 to December 2000, encompassing moderate to high solar activity phases within Solar Cycle 23. This timeframe provides sufficient temporal coverage to investigate seasonal patterns, interannual variability, and solar-cycle influences on the propagation factor M(3000)F2.

Ionosonde Data from Korhogo

The primary dataset consists of ionosonde observations from the Korhogo station (9.33°N, 5.42°W), located within the African equatorial zone. During the study period, routine ionospheric soundings produced ionograms from which standard

parameters such as foF2 and h'F2 were scaled. The M(3000)F2 values employed in this study were derived following established URSI scaling procedures and obtained from previously processed and published datasets archived in global ionospheric repositories. Daily and monthly mean values were extracted to ensure consistency and reliability.

Korhogo's location within the equatorial ionization anomaly region makes its data particularly valuable for characterizing low-latitude F2-layer behaviour in West Africa, a region with limited long-term observational coverage.

Solar Flux (F10.7) Data

Solar activity was quantified using the F10.7 cm solar radio flux index, obtained from datasets published by the National Research Council of Canada and disseminated through NOAA's Space Weather Prediction Center. The F10.7 index provides a continuous and reliable measure of solar EUV variability and is widely used in ionospheric research. Daily F10.7 values for 1993–2000 were employed to ensure temporal alignment with the ionosonde observations.

Data Resolution and Processing

Both ionospheric and solar datasets were available at daily resolution. To reduce short-term variability and mitigate the influence of data gaps, daily values were averaged to produce monthly means. This approach facilitates the analysis of diurnal behaviour, seasonal dependence (equinox versus solstice), and long-term solar-cycle modulation of M(3000)F2.

Justification for Data Selection

The selected datasets are authoritative, continuous, and well suited for equatorial ionospheric research. The 1993–2000 interval

represents a scientifically valuable period with reliable ionosonde coverage in West Africa and well-documented solar activity. Using these datasets enables meaningful comparison with previous studies across other equatorial regions and contributes to improving the understanding and modelling of African equatorial ionospheric behaviour.

Table 1: Typical sample of M(3000)F2 data

```

    ÚAAAAAAAAAAAAAAAAAAAAAAAAAAAAAAAAAAAAAAAAAAAA
    AAAAAAAAAAAAAAAAAAAAAAAAAAAAAAAAAAAAAAAAAAAAA
    AAAAA;
  
```

```

    3
    KORHOGO
    CARACTERISTIQUE: 03 M(3000)F2 3
    3
    JANVIER
  
```

```

    1996
    3
  
```

```

    AAAAAAAAAAAAAAAAAAAAAAAAAAAAAAAAAAAAAAAAAAAAA
    AAAAAAAAAAAAAAAAAAAAAAAAAAAAAAAAAAAAAAAAAAAAA
    AAAAA´
  
```

```

    3 3 0000 0100 0200 0300 0400
    0500 0600 0700 0800 0900 1000
    1100 3
    3
  
```

```

    3 1 3U330F 327 335 304F L
    L L F 324 285 264R
    U238H 3
  
```

```

    3 2 3U332F 324S 332 317S 326
    341 348 310 293 286 264G
    269G 3
  
```

```

    3 3 3 L L L L 336F
    L L 331 306 U278R U256R
    255G 3
  
```

```

    3 4 3 L 336S F L 347F
    F 361 326 329 307R 286R
    272 3
  
```

```

    3 5 3U325F 341 332 348 340
    326 F 331 310 279H 260
    260 3
  
```

```

    3 6 3 338 F L 320F L
    340F 362 326 311 268 266
    252G 3
  
```

```

    3 7 3 L L F 338 324
    F 341 324 302 277 283
    264 3
  
```

```

    3 8 3 L L L L L
    E E 326 307 274R 273R
    238 3
  
```

3 9 3	L	L	F	L	F
L S 357	316	U285R	259R		
276G 3					
3 10 3	L	L	L	L	L
L E 347	314	269R	276		
250G 3					
3 11 3	L	L	L	F	L
E E 328	303	272	262		
249G 3					
3 12 3	L	L	318S	298	336
348F E 348	327	294S			C
C 3					
3 13 3	L	349F	L	F	L
S E 348	336	331	318		
300 3					
3 14 3	325	317	308S	269	269
275 326	322	327	312	304	
273 3					
3 15 3	296	320	F	288S	272
295 309S	314	316	U301R	304	
277R 3					
3 16 3	302	L	L	L	311L
335 352	332	294	276	283	
265 3					
3 17 3	341	344F	337	L	F
293 326	337	330	307R	U256R	
263G 3					
3 18 3	340	347	341	319	330
363 E 352	367	351	326		
285 3					
3 19 3	L	L	357	343	F
U344S E 332	322	284	231G		
252G 3					
3 20 3	L	L	L	L	341
S C C C C C					
C 3					
3 21 3	323S	L	F	323	L
E S 319	289	280	263		
272G 3					
3 22 3	L	L	F	F	330F
E E 319	282	290	252		
262G 3					
3 23 3	C	C	C	C	C
C C C 290	284	273			
271G 3					
3 24 3	F	F	L	F	345
S E 348	323	U276R	276		
230 3					
3 25 3	F	L	F	L	L
S E 341	348	319R	U269R		
253G 3					
3 26 3	347S	350	328	310	320
U333S E 327	315	266	257G		
263G 3					

computed and systematically presented in tabular form. In addition, the diurnal behaviour of these regression parameters for the different seasons was illustrated through graphical plots, allowing for a detailed assessment of temporal variability in the strength and nature of the M(3000)F₂–F_{10.7} relationship.

An empirical model for M(3000)F₂ appropriate to the equatorial ionospheric environment was developed using the regression results corresponding to the highest values of R², which indicate stronger statistical dependence between M(3000)F₂ and solar flux. The use of regression-based techniques for modelling M(3000)F₂ is consistent with earlier studies; for instance, Tukhashvili et al. (2003) employed a similar approach to construct an M(3000)F₂ model using long-term ionospheric observations from a mid-latitude German station (54.38°N) covering the period 1958–1986.

The performance of the derived equatorial M(3000)F₂ model was evaluated under representative solar activity conditions corresponding to low (F_{10.7} = 70 sfu), moderate (F_{10.7} = 120 sfu), and high (F_{10.7} = 250 sfu) solar flux levels. Furthermore, model outputs were validated by comparison with observed M(3000)F₂ values obtained from another equatorial ionosonde station during periods of low solar activity (1995) and high solar activity (1991), thereby testing the model's robustness and applicability beyond the primary study location.

IV. Results

Morphology of M(3000)F₂

Figure 1 (a–d) presents the diurnal variation of seasonally averaged M(3000)F₂ for the March equinox, June solstice, September equinox, and

December solstice, using data spanning the years 1993 to 2000. Across all seasons, the observed M(3000)F₂ patterns exhibit characteristic features typical of equatorial ionospheric stations. These include a pronounced peak around sunrise, a marked depression during daytime hours, and a resurgence leading to enhanced values during the nighttime period.

The influence of diurnal variation on M(3000)F₂ is particularly strong irrespective of season. In general, a sharp maximum is observed near local sunrise (approximately 0600 LT), followed by a rapid decline in values up to about 0900 LT. The interval between late morning and late afternoon (roughly 1000–1700 LT) is dominated by a well-developed daytime trough, often exhibiting a relatively flat minimum. A distinctive post-sunset enhancement typically appears around 1800 LT, followed by a secondary minimum near 2000 LT. Subsequently, M(3000)F₂ rises steadily to reach a prominent nighttime peak. For all seasons, nighttime M(3000)F₂ values exceed those observed during daytime hours, with a substantial contrast between the two periods. Additionally, the diurnal patterns display both seasonal and solar-cycle dependence, with the daytime trough becoming increasingly pronounced as solar flux levels rise.

Figure 2 (a–h) illustrates the diurnal variation of seasonally averaged M(3000)F₂ for individual years from 1993 to 2000. Distinct seasonal differences are evident across all years, with equinoctial periods consistently exhibiting higher M(3000)F₂ values than solstitial periods. Nighttime behaviour is characterized by a gradual and sustained increase in M(3000)F₂ following sunset. Seasonal contrasts are particularly noticeable during nighttime hours under low and moderate

solar activity conditions, especially immediately after sunset.

A notable feature is the pronounced disparity in $M(3000)F_2$ values around sunset during the June solstice when compared with other seasons. Overall, the results indicate an inverse dependence of $M(3000)F_2$ on solar activity. Lower $M(3000)F_2$ values are observed during years of high solar activity (1999 and 2000), when $F_{10.7}$ exceeds 150 sfu. Intermediate values occur during moderate solar activity years such as 1993 and 1998, corresponding to $F_{10.7}$ levels between 100 and 150 sfu. In contrast, the highest $M(3000)F_2$ values are recorded during low solar activity years (1994–1997), when $F_{10.7}$ remains below 100 sfu.

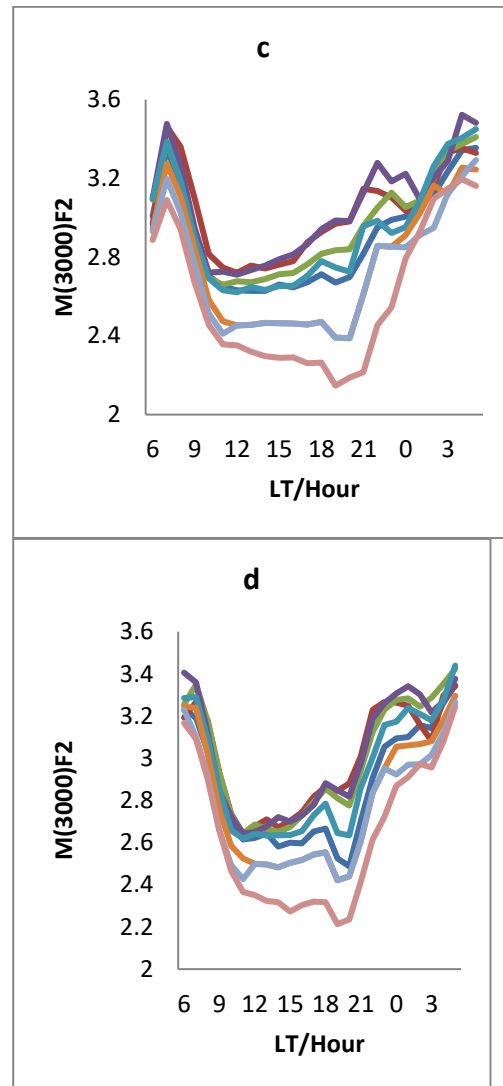
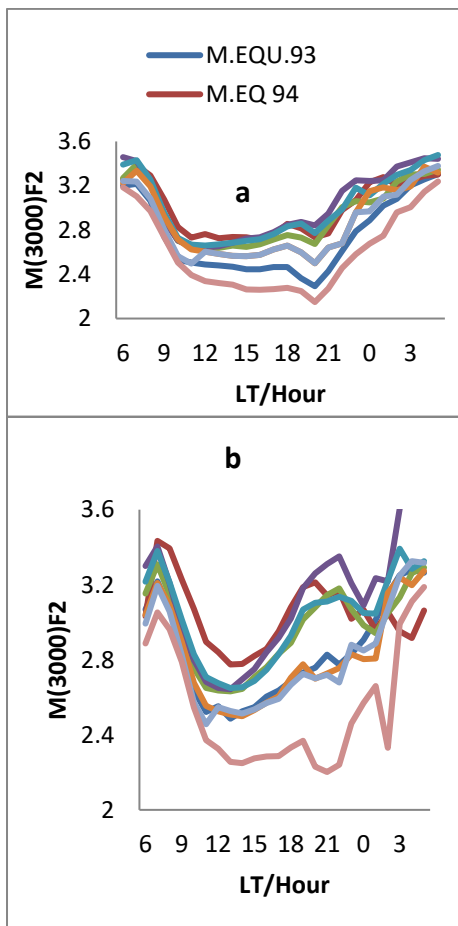
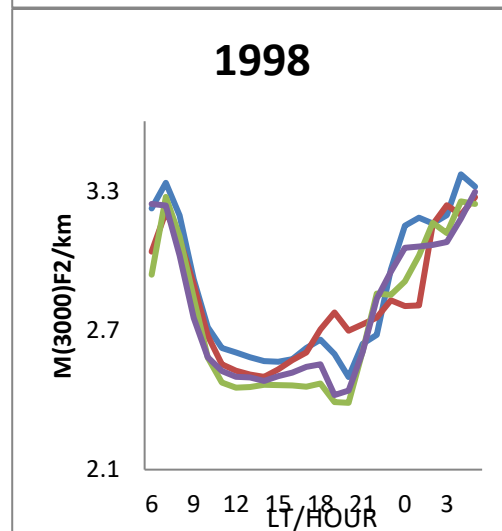
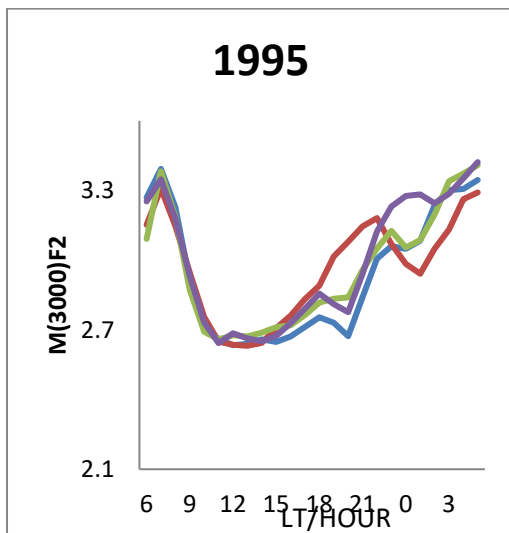
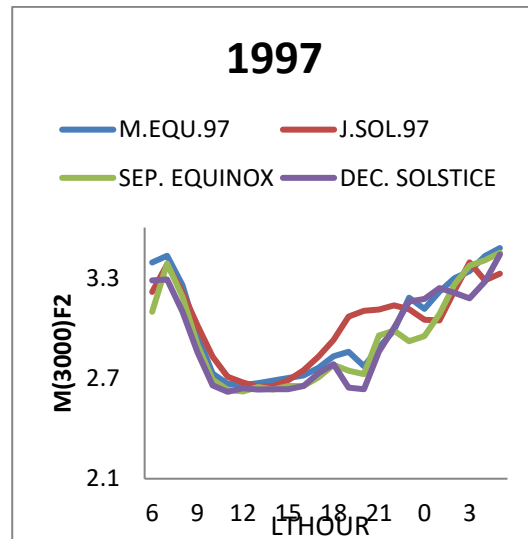
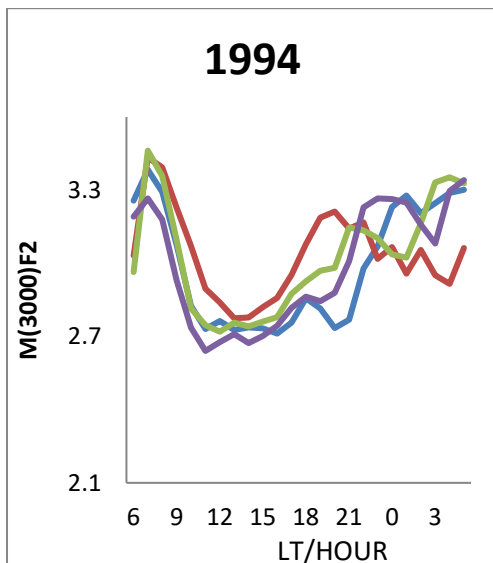
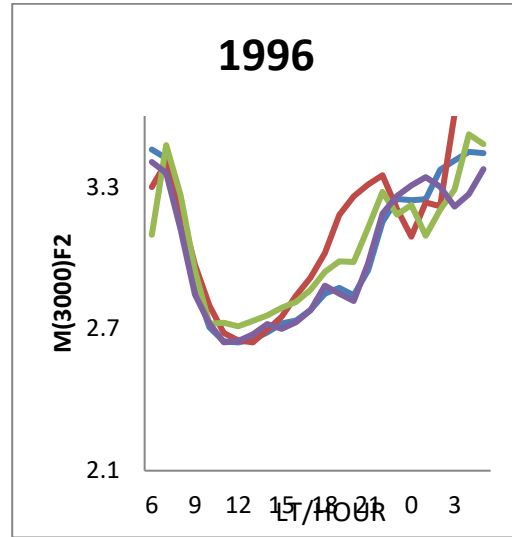
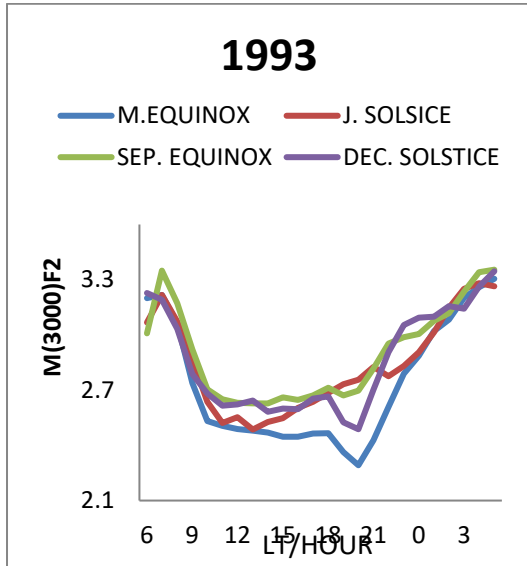


Figure 1: The diurnal plot of $M(3000)F_2$ for (a) March equinox, (b) June solstice, (c) September equinox, and (d) December solstice over the years of study, 1993 - 2000



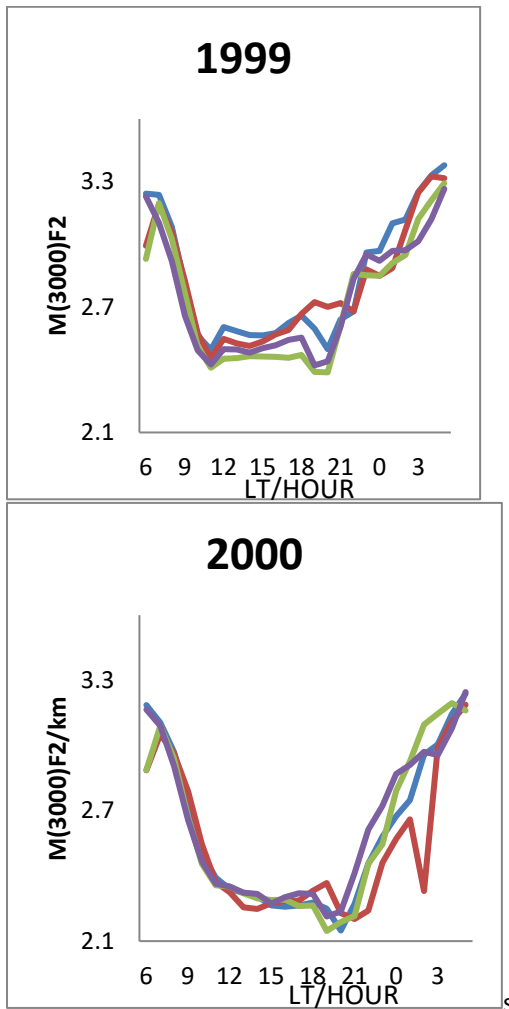


Figure 2: Diurnal plot of seasonal average of $M(3000)F2$ for the four seasons over the years (a) 1993 , (b) 1994 , (c) 1995, (d) 1996 (e) 1997, (f) 1998, (g) 1999, and (h) 2000

Linear Regression Analysis

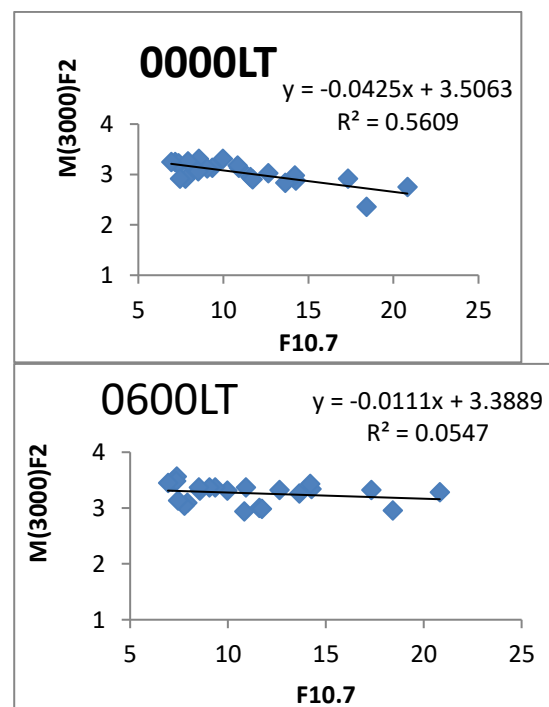
Figures 3–6 illustrate the linear regression relationships between $M(3000)F2$ and the solar radio flux index $F10.7$ for all seasons during the period 1993–2000. The regression outcomes are organized and discussed according to seasonal classifications. Overall, the analysis reveals a clear inverse dependence of $M(3000)F2$ on solar activity, as represented by $F10.7$, across all seasons.

The coefficients of determination (R^2) indicate a strong statistical relationship between

$M(3000)F2$ and $F10.7$, particularly during daytime and early nighttime hours, spanning approximately 0700 LT to 2100 LT. For all seasonal categories, the regression slopes are consistently negative, confirming that increases in solar flux are associated with corresponding decreases in $M(3000)F2$ values.

Quantitatively, the regression slopes for the equinoctial seasons vary between -0.029 and -0.032 (sfu^{-1}), while those for the solstitial seasons range from -0.029 to -0.027 (sfu^{-1}). The regression intercepts fall within the interval of 2.917 to 2.924 for the equinoxes, and between 2.903 and 2.924 for the solstices. These relatively narrow ranges of slope and intercept values suggest a stable and consistent response of $M(3000)F2$ to variations in solar flux, regardless of seasonal differences.

March Equinox



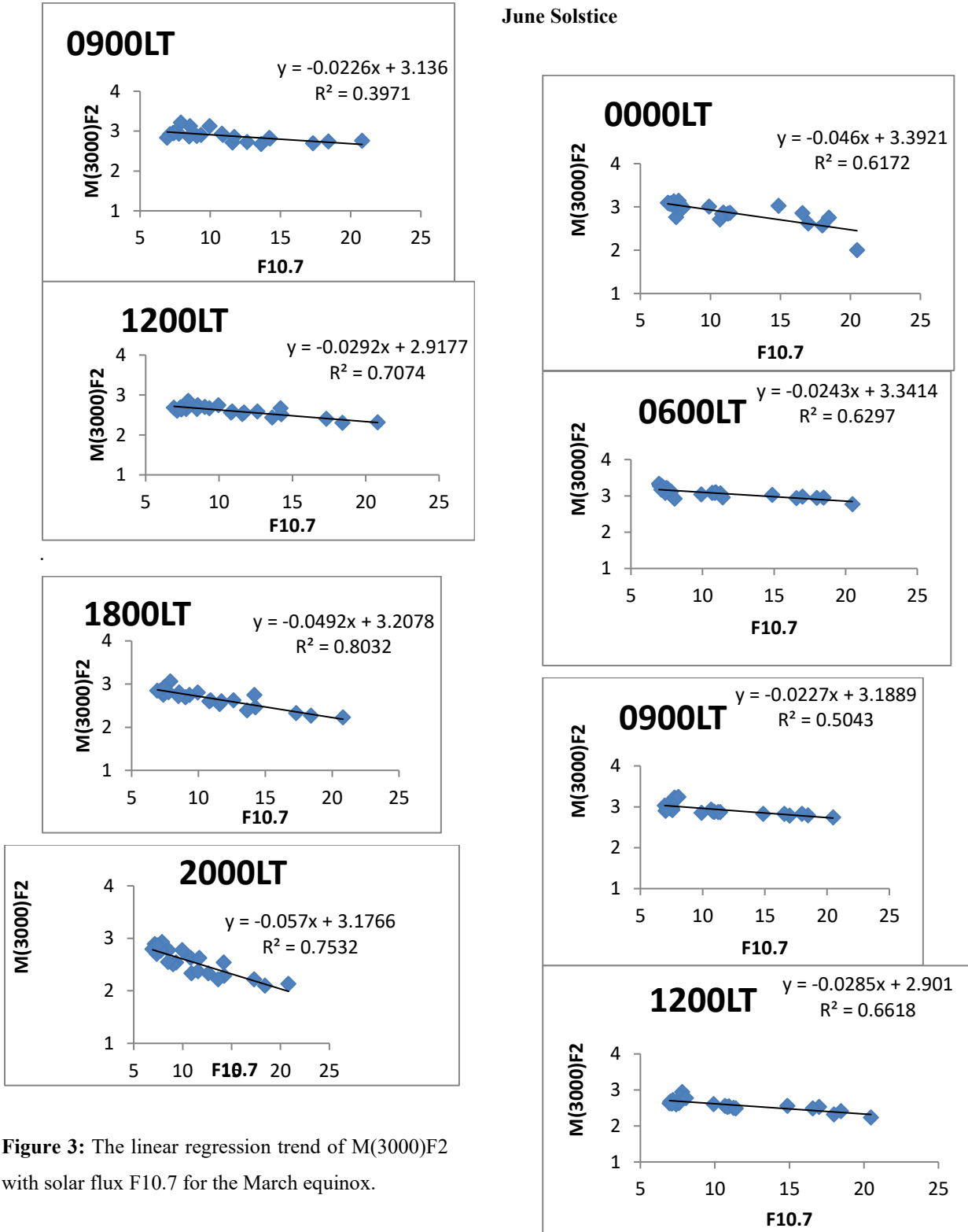


Figure 3: The linear regression trend of M(3000)F2 with solar flux F10.7 for the March equinox.

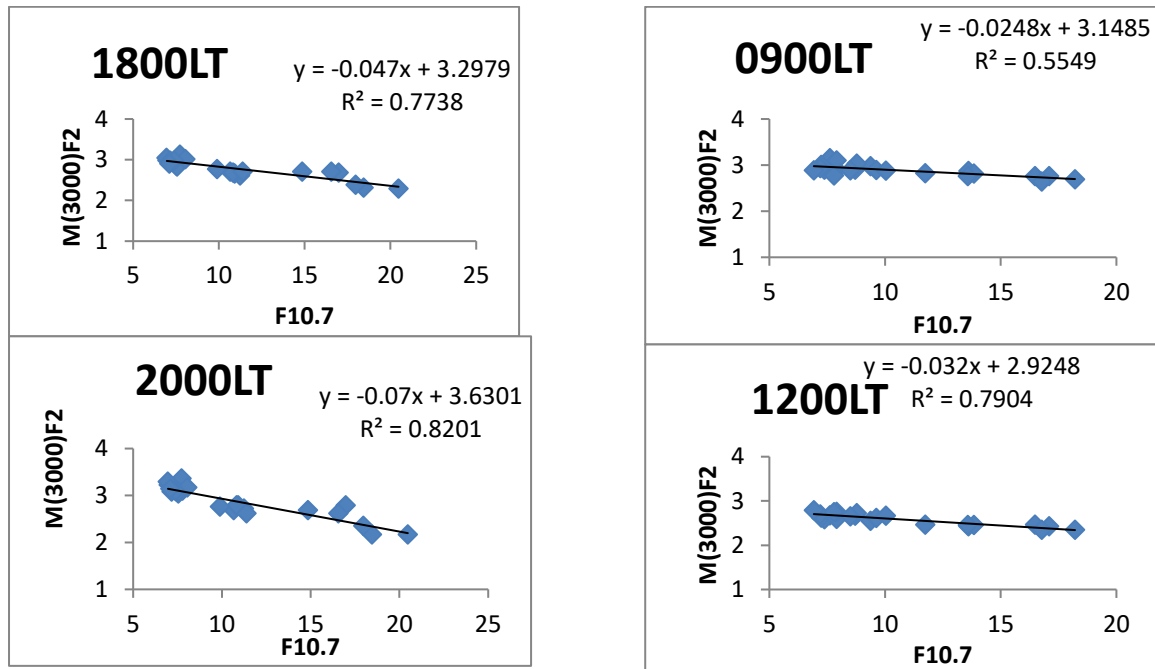


Figure 4: The linear regression trend of M(3000)F2 with solar flux F10.7 for June solstice.

September Equinox

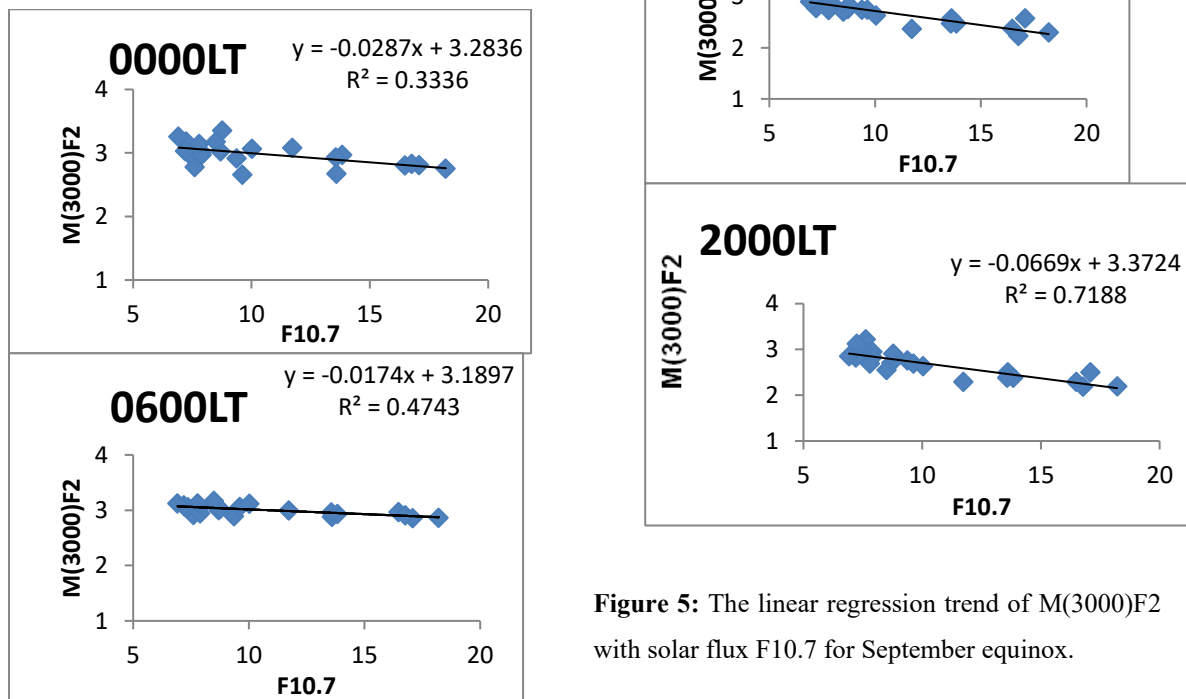


Figure 5: The linear regression trend of M(3000)F2 with solar flux F10.7 for September equinox.

December Solstice

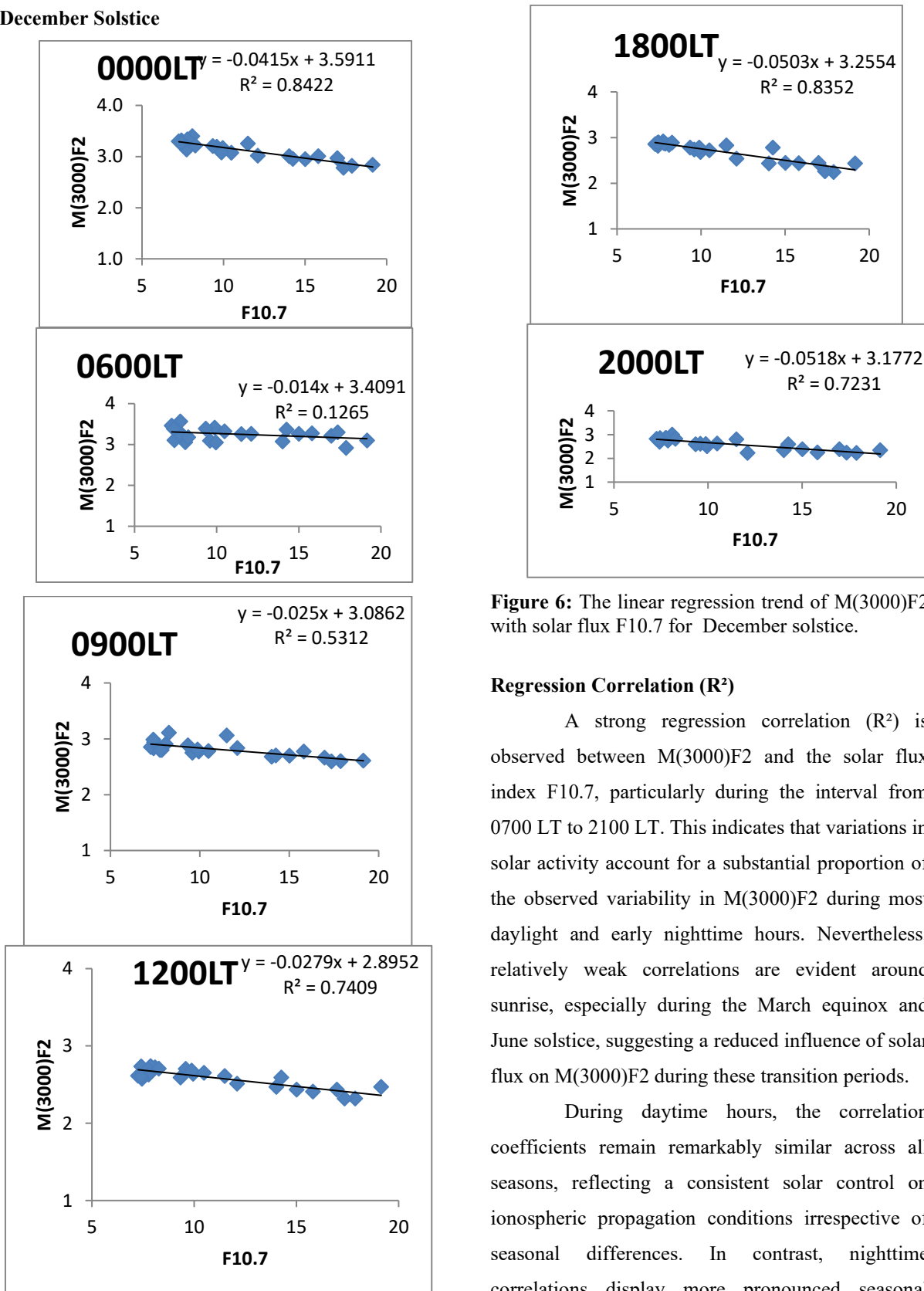


Figure 6: The linear regression trend of M(3000)F2 with solar flux F10.7 for December solstice.

Regression Correlation (R²)

A strong regression correlation (R²) is observed between M(3000)F2 and the solar flux index F10.7, particularly during the interval from 0700 LT to 2100 LT. This indicates that variations in solar activity account for a substantial proportion of the observed variability in M(3000)F2 during most daylight and early nighttime hours. Nevertheless, relatively weak correlations are evident around sunrise, especially during the March equinox and June solstice, suggesting a reduced influence of solar flux on M(3000)F2 during these transition periods.

During daytime hours, the correlation coefficients remain remarkably similar across all seasons, reflecting a consistent solar control on ionospheric propagation conditions irrespective of seasonal differences. In contrast, nighttime correlations display more pronounced seasonal variability, highlighting the increasing role of non-

solar drivers such as electrodynamic processes, neutral winds, and recombination effects after sunset.

Figure 7 presents the diurnal variation of the regression correlation (R^2) for all seasons. In general, the strength of the correlation is higher during the daytime than at night. The maximum correlation values occur shortly after sunrise, around 0700 LT, indicating a period when solar forcing exerts a dominant influence on the F2-layer propagation factor. Conversely, the minimum correlation values are clearly observed near sunrise during the June solstice and March equinox. Overall, seasonal differences in R^2 are more prominent during nighttime hours than during daytime, further emphasizing the complex interplay of solar and dynamical processes governing equatorial ionospheric behavior.

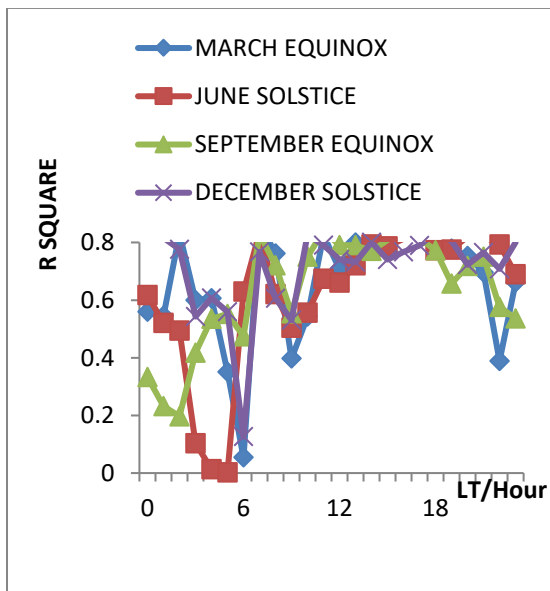


Figure7:The diurnal plot of the regression correlation, R^2 for all the seasons.

The Regression Slope (a)

In general, M(3000)F2 exhibits an inverse relationship with the solar flux index F10.7 across all the seasons considered in this study. This

indicates that increases in solar activity are consistently associated with a reduction in the value of the M(3000)F2 propagation factor, irrespective of seasonal conditions. Figure 8 illustrates the diurnal variation of the regression slope between M(3000)F2 and F10.7 for the different seasons.

The slope values obtained for all seasons fall within the range of -0.001 (sfu) $^{-1}$ to -0.006 (sfu) $^{-1}$, further confirming the negative dependence of M(3000)F2 on solar flux. During daytime hours, the slope variations are largely comparable across seasons, suggesting a uniform solar influence on the ionospheric F2 layer during periods of direct solar illumination. In contrast, nighttime slopes show noticeable inconsistencies from one season to another, reflecting the growing influence of seasonal electrodynamic processes, thermospheric winds, and recombination effects after sunset, which modify the ionospheric response to solar activity.

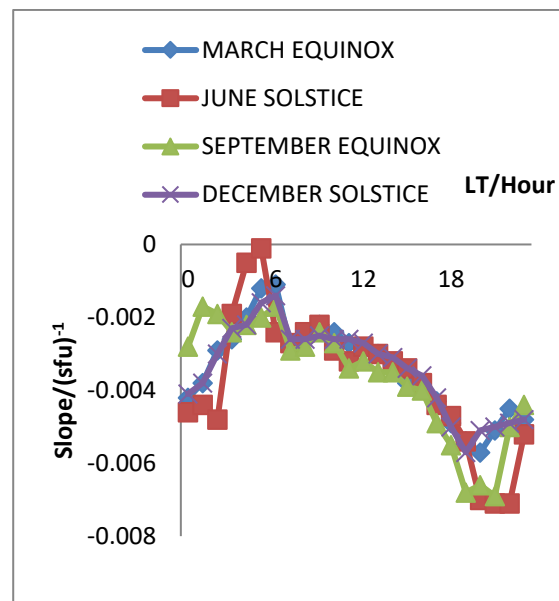


Figure8:The diurnal plot of slope for all the seasons

The Regression Intercept (b)

Figure 9 presents the diurnal variation of the regression intercept for the different seasons. The pattern of the intercept is generally similar across all

seasons from sunrise (0600 LT) to sunset (1800 LT). Within this period, the intercept exhibits a daytime trough, while higher values occur during the nighttime, forming distinct crests. Seasonal differences are minimal during the daytime but become noticeable at night.

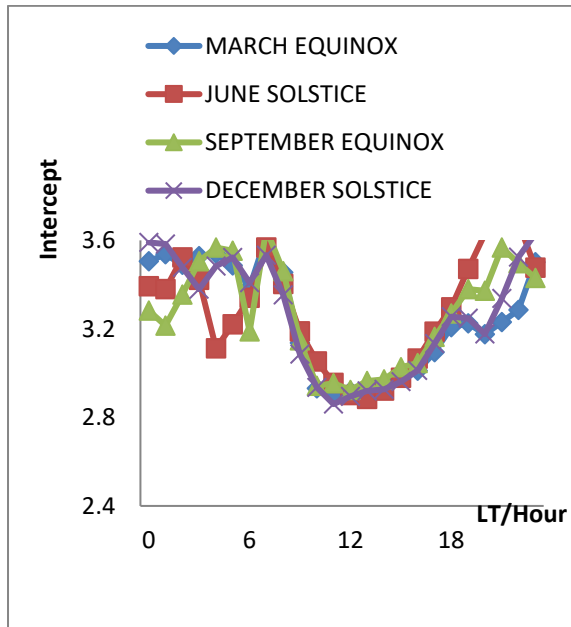


Figure 9: The diurnal plot of Intercept for all the seasons.

The intercept values for the different seasons fall within the following ranges: March equinox (2.93–3.62), June solstice (2.92–3.67), September equinox (2.94–3.65), and December solstice (2.86–3.63). These ranges indicate that the highest intercept peak occurs during the June solstice, followed closely by the September equinox, December solstice, and March equinox. In contrast, the lowest intercept values are recorded during the December solstice, followed sequentially by the June solstice, March equinox, and September equinox.

V. Discussion

Morphology of M(3000)F2

The observed diurnal and seasonal patterns of M(3000)F2 over Korhogo from 1993 to 2000 closely align with established characteristics of the equatorial ionosphere, particularly for stations located within or near the Equatorial Ionization Anomaly (EIA). The recurring features of a sharp enhancement at sunrise, a pronounced daytime minimum, and elevated nighttime values across all seasons are consistent with classical descriptions of F₂-layer behaviour at low latitudes¹. The pronounced morning peak around 0600 LT is associated with the rapid buildup of electron density following the onset of solar photoionization, as solar radiation increases sharply after sunrise. This behaviour accords with Chapman theory, which predicts a rapid rise in ionization as the solar zenith angle decreases²¹.

The rapid reduction in M(3000)F2 following sunrise until approximately 0900 LT suggests a lowering of hmF₂ driven by intensified downward plasma diffusion and increased ion-neutral collision frequencies as solar heating becomes more effective. Comparable early-morning depressions in F₂-layer parameters have been documented at other West African stations, including Ouagadougou and Lagos^{8,29}, indicating that this feature is a common regional characteristic.

The well-defined daytime trough observed between 1000 LT and 1700 LT reflects a period during which the F₂ layer remains relatively stable under strong solar ionization and reduced vertical plasma drift. In equatorial regions, the suppression of upward $E \times B$ drift during midday results in a reduction in hmF₂, leading to lower MUF values and, consequently, reduced M(3000)F2. This behaviour is consistent with established descriptions

of equatorial electrodynamics^{25,9}. The consistently “flat-bottomed” nature of the trough across all seasons suggests extended intervals of minimal vertical displacement of the F₂ layer during daylight hours.

The post-sunset enhancement observed around 1800 LT represents a well-known manifestation of the equatorial pre-reversal enhancement (PRE). This phenomenon arises from the intensification of the eastward electric field at dusk, which drives strong upward plasma drifts and elevates the F₂ layer to higher altitudes⁹. The resulting increase in hmF₂ enhances the MUF and, by extension, M(3000)F₂. The Korhogo observations are consistent with earlier results reported for other West African stations^{7,20}, reinforcing the importance of PRE in shaping evening ionospheric propagation conditions within this longitude sector.

The prominent nighttime maxima recorded in all seasons reflect reduced recombination effects and diminished ion-neutral drag following the absence of solar ionization. Given the strong dependence of M(3000)F₂ on hmF₂ and the electron density profile, elevated nighttime hmF₂ values naturally produce higher propagation factor values. The persistence of nighttime enhancement throughout the study period highlights the dominant role of diurnal forcing on F₂-layer structure at equatorial latitudes.

Seasonal differences, notably higher M(3000)F₂ values during equinoxes compared to solstices, are consistent with previous equatorial investigations^{8,6}. During equinoctial periods, more symmetric solar illumination strengthens the fountain effect, resulting in enhanced plasma uplift and increased ionization crests. The associated

increases in hmF₂ and NmF₂ directly translate into higher MUF and M(3000)F₂ values. Conversely, the deeper troughs observed during the June solstice, particularly near sunset, may be linked to seasonal weakening of PRE driven by changes in thermospheric wind patterns¹⁵. Overall, the morphology documented for the 1993–2000 interval confirms that Korhogo exhibits behaviour typical of an African equatorial ionospheric station.

Year-to-Year Variations

Interannual analysis spanning 1993 to 2000 reveals a clear sensitivity of M(3000)F₂ to solar cycle variability. The results show that the lowest M(3000)F₂ values occur during years of high solar activity (1999–2000), moderate values during intermediate activity years (1993 and 1998), and the highest values during periods of low solar activity (1994–1997). This inverse dependence is consistent with expected equatorial F₂-layer responses under enhanced solar EUV forcing. During high solar activity, increased EUV radiation significantly raises ion production and NmF₂ but simultaneously leads to a reduction in hmF₂ due to intensified thermal contraction and increased ion-neutral collisions. Since M(3000)F₂ is strongly controlled by hmF₂, the lowering of the F₂ layer during high solar activity results in reduced propagation factor values. Similar inverse relationships between hmF₂ and solar flux have been reported in both global and African studies^{5,32,20}. Consequently, the long-term variations identified in this study provide strong empirical support for the established understanding that enhanced solar flux compresses the equatorial F₂ layer, leading to lower M(3000)F₂ values.

Linear Regression Relationship between M(3000)F₂ and F10.7

The regression analysis reveals consistently negative slopes for all seasons, confirming an inverse relationship between M(3000)F₂ and solar

flux (F10.7). This outcome is in agreement with previous findings from equatorial and low-latitude regions in Africa and elsewhere^{28,9,30}. The reported slope values, approximately -0.001 to -0.006 sfu⁻¹, indicate that increases in solar flux are associated with systematic decreases in the propagation factor, reflecting the lowering of the F₂ layer under strong EUV radiation. The regression intercepts, which range between 2.86 and 3.67, are consistent with theoretical expectations for equatorial MUF-to-foF₂ ratios. The occurrence of higher intercept values at night reflects post-dusk elevation of hmF₂. The seasonal ranking of intercept magnitudes, with the June solstice exhibiting the highest values, suggests enhanced influence of nighttime thermospheric winds during solstice conditions, in line with equatorial electrodynamic theory²⁶.

The strong regression correlation coefficients (R²), particularly between 0700 LT and 2100 LT, indicate that solar flux exerts a dominant and predictable control on ionospheric behaviour during daylight hours. This observation is consistent with earlier findings that F10.7 has its strongest predictive influence on foF₂ and hmF₂ during the daytime in equatorial regions³². The weaker correlations observed around sunrise during the March equinox and June solstice likely reflect the influence of transient electrodynamic processes, including rapid changes in vertical plasma drift and recombination rates. Overall, the consistency of regression parameters across seasons and years demonstrates that solar flux serves as a reliable predictor of M(3000)F₂ variability in the African equatorial sector, supporting the development of region-specific predictive models.

Interpretation of Regression Parameters (Slope, Intercept, R²)

Regression slope (a):

The negative slope values confirm that increased solar radiation leads to compression of the

F₂ layer, lowering hmF₂ and reducing both MUF and the propagation factor. The similarity of slope behaviour across seasons during daytime hours suggests that solar forcing outweighs seasonal electrodynamic influences during this period, consistent with findings³³.

Regression intercept (b):

The recurring pattern of daytime minima and nighttime maxima in the intercept highlights the strong diurnal influence of electric fields and thermospheric winds on hmF₂. Seasonal variations observed at night reflect differences in PRE intensity and wind-driven lifting throughout the year.

Regression correlation (R²):

High daytime correlation values emphasize the deterministic role of solar activity in controlling ionospheric conditions. In contrast, reduced correlations during nighttime and around sunrise indicate the growing influence of complex electrodynamic processes, such as PRE, $E \times B$ drifts, and nighttime recombination, which can obscure the direct effects of solar forcing.

Overall, the results demonstrate that M(3000)F₂ over Korhogo exhibits well-defined diurnal and seasonal patterns shaped by the combined effects of solar radiation, equatorial electrodynamic processes, and thermospheric dynamics. The consistent sunrise peak, midday depression, post-sunset enhancement, and nighttime maximum observed throughout the study period reaffirm the characteristic behaviour of the equatorial F₂ layer and validate established mechanisms involving photoionization, vertical plasma transport, and recombination processes.

The analysis further confirms that M(3000)F₂ is strongly influenced by solar activity, with increased solar flux producing lower

propagation factor values. The negative regression slopes obtained across all seasons and years demonstrate that enhanced EUV radiation during periods of high solar activity compresses the F₂ layer, thereby reducing the maximum usable frequency for long-distance HF communication. This inverse relationship is persistent, statistically robust, and consistent with earlier empirical studies. Additionally, the strong daytime correlation between M(3000)F₂ and F_{10.7} underscores the dominant role of solar forcing in determining ionospheric propagation conditions in the African equatorial region. Seasonal variations in early morning and nighttime correlations further highlight the role of PRE, thermospheric winds, and other electrodynamic processes unique to equatorial latitudes.

In summary, this study provides important insights into the behaviour of the propagation factor M(3000)F₂ in a relatively underrepresented African sector, enhances understanding of solar–ionospheric coupling at low latitudes, and underscores the value of long-term observational datasets for improving ionospheric modelling and HF communication planning.

Recommendations

Based on the outcomes of this investigation, the following recommendations are advanced:

1. **Strengthen ionospheric monitoring across West Africa:** Additional ionosonde stations should be deployed along the West African equatorial zone to supplement observations from Korhogo and enhance spatial resolution for the assessment of M(3000)F₂ and other key ionospheric parameters.
2. **Adopt a multi-instrument observational approach:** Ionosonde data should be integrated with GNSS-based Total Electron Content

(TEC), ground magnetometer measurements, and atmospheric wind observations in order to achieve a more holistic understanding of equatorial electrodynamic processes affecting M(3000)F₂.

3. **Enhance ionospheric and HF propagation models:** The empirical findings of this study should be incorporated into regional and global ionospheric models, including IRI, NeQuick, and SUPIM, which frequently show reduced performance over African equatorial latitudes.
4. **Optimize HF communication frequency management:** HF communication operators, particularly within the military, aviation, and broadcasting sectors, should implement seasonal and solar-activity–dependent frequency planning strategies that account for the pronounced diurnal and solar-driven variability of M(3000)F₂.
5. **Reinforce space-weather early warning capabilities:** Space-weather monitoring agencies should integrate F_{10.7} threshold levels identified in this study into operational warning systems to better anticipate periods of HF communication disruption associated with elevated solar activity.
6. **Preserve and digitize historical ionospheric records:** Research institutions in Africa should prioritize the digitization and archiving of historical ionograms and ionospheric datasets to support long-term climatological analyses and improve the reliability of future modelling efforts.
7. **Encourage regional and international research collaboration:** Collaborative efforts between African ionospheric research groups and international organizations such as GIRO, SWPC, and SCOSTEP should be strengthened to promote data sharing, instrument standardization, and coordinated studies of solar–ionosphere coupling.

Acknowledgments

The researcher sincerely appreciates the National Resource Canada group for making available the solar flux f10.7 data at <http://www.spaceweather.ca/solarflux/sx-5-en.php>.

The M(3000)F2 data used in this work can be accessed through <http://eprints.lmu.edu.ng/2918/>.

The researcher sincerely appreciates the Tertiary Education Trust Fund (TETFUND) for providing the financial support that made this research possible. The sponsorship greatly facilitated the successful execution of this study and contributed significantly to its overall quality and impact.

Profound gratitude is also extended to the Management of Kwara State College of Education, Oro, for granting the opportunity, institutional support, and enabling environment required to carry out this work. Their encouragement and commitment to academic development remains deeply valued.

References

- [1] Rishbeth, H., & Mendillo, M. (2001). Patterns of ionospheric variability. *Journal of Atmospheric and Solar-Terrestrial Physics*, 63(15), 1661–1680.
- [2] Davies, K. (1990). Ionospheric radio. Peter Peregrinus Ltd.
- [3] Zolesi, B., & Cander, L. R. (2014). Ionospheric prediction and forecasting. Springer.
- [4] Tapping, K. F. (2013). The 10.7 cm solar radio flux (F10.7). *Space Weather*, 11(7), 394–406.
- [5] Liu, L., Wan, W., Chen, Y., & Le, H. (2006). Solar activity variability of ionospheric peak electron density. *Journal of Geophysical Research: Space Physics*, 111(A08304).
- [6] Obrou, O., Zoundi, C., Tchinda, P., & Fambitakoye, O. (2009). Seasonal ionospheric variations in West Africa. *Journal of Atmospheric and Solar-Terrestrial Physics*, 71(3–4), 195–205.
- [7] Obrou, O., Zoundi, C., Tchinda, P., & Fambitakoye, O. (2003). Sunset enhancement in hmF2 over Korhogo. *Annales Geophysicae*, 21(10), 2087–2096.
- [8] Adeniyi, J. O., Radicella, S. M., & Adimula, I. A. (2014). Equatorial ionospheric variations: Comparison of African and European regions. *Advances in Space Research*, 54(4), 495–505.
- [9] Anderson, D., Heelis, R., & Hanson, W. (2004). The equatorial pre-reversal enhancement: Results from the Jicamarca radar. *Journal of Geophysical Research: Space Physics*, 109(A02303).
- [10] Hargreaves, J. K. (1992). The solar-terrestrial environment. Cambridge University Press.
- [11] Schunk, R. W., & Nagy, A. F. (2009). Ionospheres: Physics, plasma physics, and chemistry. Cambridge University Press.
- [12] Bilitza, D. (2018). The International Reference Ionosphere – Status and future improvements. *Journal of Atmospheric and Solar-Terrestrial Physics*, 179, 7–25.
- [13] Goodman, J. M. (2005). Operational communication theory and performance. Artech House.
- [14] Chen, Y., Liu, L., Wan, W., & Ning, B. (2011). Solar activity dependence of the ionospheric peak electron density. *Journal of Atmospheric and Solar-Terrestrial Physics*, 73(1), 87–95.
- [15] Stolle, C., Lühr, H., & Rother, M. (2008). The equatorial ionization anomaly and electrodynamics. *Annales Geophysicae*, 26(2), 389–406.
- [16] Abdu, M. A. (2016). Equatorial ionosphere-thermosphere system: Electrodynamics and irregularities. *Advances in Space Research*, 57(5), 1105–1122.
- [17] Hsu, C. T., Fang, T. W., & Wang, W. (2008). Effects of equatorial electrojet on F region. *Journal of Geophysical Research: Space Physics*, 113(A01311).
- [18] Oladipo, O. A., Adebisi, S. J., & Gyamfi, J. (2014). Longitudinal ionospheric irregularities over African equatorial sector. *Advances in Space Research*, 54(9), 1908–1918.
- [19] Adebisi, S. J., Adebisi, A. A., & Oladipo, O. A. (2015). Seasonal ionospheric variations at equatorial and low-latitude African stations. *Journal of Atmospheric and Solar-Terrestrial Physics*, 130, 123–132.
- [20] Adebisi, B. O., Rabi, A. B., & Adeniyi, J. A. (2013). Variability of ionospheric parameters over an equatorial station in Africa and evaluation of the IRI-2012 model. *Journal of Atmospheric and Solar-Terrestrial Physics*, 100–101, 10–18.
- [21] Chapman, S. (1931). The absorption and dissociative or ionizing effect of monochromatic radiation. *Proceedings of the Physical Society*, 43(26), 26–45.
- [22] Ratcliffe, J. A. (1972). An introduction to the ionosphere and magnetosphere. Cambridge University Press.

- [23] Tsurutani, B. T., Mannucci, A. J., Iijima, B. A., & Saito, A. (2009). Ionospheric storms and solar activity. *Journal of Space Weather and Space Climate*, 1(A01), 1–8.
- [24] Lastovicka, J. (2006). Forcing of the ionosphere by solar and geomagnetic activity. *Journal of Atmospheric and Solar-Terrestrial Physics*, 68(3), 179–187.
- [25] Fejer, B. G., Scherliess, L., & de Paula, E. R. (1999). Effects of the vertical drift velocity on equatorial F region plasma irregularities. *Journal of Geophysical Research: Space Physics*, 104(A4), 6829–6842.
- [26] Kelley, M. C. (2009). *The Earth's ionosphere: Plasma physics and electrodynamics*. Academic Press.
- [27] Arowolo, O. A., & Adeniyi, J. O. (2016). Assessment of IRI-2012 hmF2 option over an equatorial station. *Annales Geophysicae*, 34(5), 403–414.
- [28] Adeniyi, J. O. (1996). Nighttime ionospheric electron density profiles at the magnetic equator during solar minimum. *Radio Science*, 31(4), 955–963.
- [29] Oyekola, O. S. (2013). Variations of the M(3000)F2 parameter over an equatorial station in Nigeria. *Indian Journal of Radio and Space Physics*, 42, 284–291.
- [30] Uwamahoro, J., & Habarulema, J. (2010). Prediction of ionospheric F2 region parameters using neural networks over East Africa. *Journal of Atmospheric and Solar-Terrestrial Physics*, 72(11–12), 838–846.
- [31] Zakharenkova, I., Cherniak, I., & Krankowski, A. (2015). Global ionosonde observations of solar activity effects. *Journal of Geophysical Research: Space Physics*, 120(8), 7028–7046.
- [32] Danilov, A. D., & Lastovicka, J. (2012). Effects of solar activity on the ionospheric F2 region. *Journal of Atmospheric and Solar-Terrestrial Physics*, 90–91, 12–25.
- [33] Tukhashvili, D., Kharshiladze, O., Jandieri, G., & Diasamidze, G. (2003). Modeling and prediction of the ionospheric propagation factor M(3000)F2 using regression techniques. *Radio Science*, 38(6), 1093. <https://doi.org/10.1029/2002RS002737>